Lab on a Chip

Accepted Manuscript

ROYAL SOCIETY OF CHEMISTRY

www.rsc.org/loc

ARTICLE TYPE www. rsc.org/xxxxxx | XXXXXXXX

Oxygen control with microfluidics

Martin D. Brennan,*[a] Megan Rexius,[a] Laura Jane Elgass,[a] and David T. Eddington[a]

Received Xth XXXXXXXXXX 20XX, Accepted Xth XXXXXXXXX 20XX
First published on the web Xth XXXXXXXXXX 200X
DOI: 10.1039/b000000x

Cellular function and behavior are affected by the partial pressure of O_2, or oxygen tension, in the microenvironment. The level of oxygenation is important, as it is a balance of oxygen availability and oxygen consumption that is necessary to maintain normoxia. Changes in oxygen tension, from above physiological oxygen tension (hyperoxia) to below physiological levels (hypoxia) or even complete absence of oxygen (anoxia), trigger potent biological responses. For instance, hypoxia has been shown to support the maintenance and promote proliferation of regenerative stem and progenitor cells. Paradoxically, hypoxia also contributes to the development of pathological conditions including systemic inflammatory response, tumorigenesis, and cardiovascular disease, such as ischemic heart disease and pulmonary hypertension. Current methods to study cellular behavior in low levels of oxygen tension include hypoxia workstations and hypoxia chambers. These culture systems do not provide oxygen gradients that are found in vivo or precise control at the microscale. Microfluidic platforms have been developed to overcome the inherent limits of these current methods, including lack of spatial control, slow equilibration, and unachievable or difficult coupling to live-cell microscopy. The various applications made possible by microfluidic systems are the topic of this review. In order to understand how the microscale can be leveraged for oxygen control of cells and tissues within microfluidic systems, some background understanding of diffusion, solubility, and transport at the microscale will be presented in addition to a discussion on the methods for measuring the oxygen tension in microfluidic channels. Finally the various methods for oxygen control within microfluidic platforms will be discussed including devices that rely on diffusion from liquid or gas, utilizing on-or-off-chip mixers, leveraging cellular oxygen uptake to deplete the oxygen, relying on chemical reactions in channels to generate oxygen gradients in a device, and electrolytic reactions to produce oxygen directly on chip.

1 Need and motivation for oxygen control

Cellular function and behavior are affected by the partial pressure of oxygen, or oxygen tension, in the microenvironment. Oxygen tension impacts a variety of vital biological processes including but not limited to embryonic development, metabolism, and angiogenesis. Despite this fact, oxygen tension is an often overlooked aspect of *in vitro* systems aiming to reconstruct physiologically realistic microenvironments. Even in standard cell culture, physiologic oxygen tension is largely disregarded. Incubators maintain cells at 37°C in 5% CO_2 (to buffer the pH of cell culture media) and balanced air. The balanced air consists of approximately 21% oxygen. However, the use of an ambient level of 21% oxygen in cell culture does not reflect the range of oxygen tensions found normally in the cells and tissues of the human body. Normoxia, the term for the normal level of oxygen, is 21% in the earth's atmosphere; we typically breathe a 21% oxygen gas mixture. In physiological contexts, normoxia in cells and tissues (Table 1) is well below ambient atmospheric oxygen tension, typically falling between 2–9%[1]. Even in the most oxygenated parts of the body—the arteries, lungs, and liver—normoxia is only between 10–13%[2], so 21% oxygen is actually hyperoxic or above physiological oxygen concentrations. Other tissue-specific oxygen levels include 5% in venous blood[3], 1–7% in bone marrow[4], 0.5–7% in the brain[5], and 1% in cartilage[4].

Table 1 The physiologic oxygen levels vary for different human tissues. The indicated normoxic levels are all below atmospheric (21%) oxygen. Values compiled from refs. 3–5.

Tissue	Physiologic Oxygen (%)
Lung alveoli	13
Liver	10–13
Arterial blood	10–13
Venous blood	5
Bone marrow	0.5-7
Brain	0.5–7
Cartilage	1

The level of oxygenation is important, as it is a balance of oxygen availability and oxygen consumption that is necessary to maintain normoxia. Changes in oxygen tension, from above physiological oxygen tension (hyperoxia) to below physiological levels (hypoxia) or even complete absence of oxygen (anoxia), trigger potent biological responses. For instance, hy-

† These authors contributed equally.
[a] *UIC Bioengineering (MC 563), 820 S Wood St W103 CSN, Chicago, IL 60612. E-mail: mbrenn3@uic.edu*

poxia has been shown to support the maintenance and promote proliferation of regenerative stem and progenitor cells [1,2,6,7]. Paradoxically, hypoxia also contributes to the development of pathological conditions including systemic inflammatory response, tumorigenesis, and cardiovascular disease, such as ischemic heart disease and pulmonary hypertension.

Research has shown that a reduction in oxygen tension results in extensive alterations in gene expression. A vast array of hypoxia-related cell signaling pathways can be activated, including those for angiogenesis, metabolism, migration, proliferation, differentiation, and apoptosis. Virtually all known hypoxia-related alterations in gene expression rely on the transcriptional activity of hypoxia inducible factors (HIF) [8]. The HIF family of transcription factors includes three known isoforms of α subunits: HIF-1α, HIF-2α, and HIF-3α. Of these isoforms, HIF-1α regulation has been best characterized [9]. The HIF-1α subunit is continuously synthesized and degraded under normoxic conditions. The degradation of HIF-1α is, in fact, oxygen dependent as oxygen activates prolyl hydroxylase (PHD) enzymes. These hydroxylated proline residues facilitate the binding of a ubiquitin-protein ligase complex to HIF-1α which results in the poly-ubiquitination of HIF-1α and its proteasomal degradation. Following exposure to hypoxic conditions, HIF-1α accumulates rapidly. HIF-1α is stabilized and enters the nucleus where it heterodimerizes with the non-regulated subunit HIF-1β and initiates downstream transcription. The α subunit's nuclear translocation, accumulation, and heterodimerization with the β subunit is crucial to HIF transcriptional activity.

Current methods to study cellular behavior in low levels of oxygen tension include hypoxia workstations and hypoxia chambers. As we will describe in detail, these culture systems do not provide oxygen gradients that are found *in vivo* or control at the microscale. To fulfill this unmet need, a variety of microfluidic devices have been developed to permit tight control of oxygen levels in cultured cells. Microfluidics provides an excellent platform for studying the effect of oxygen concentration on the cellular microenvironment. In order to understand how the microscale can be leveraged for oxygen control of cells and tissues within microfluidic systems, some background understanding of diffusion, solubility, and transport at the microscale is necessary.

2 Diffusion, solubility, and transport of oxygen in microfluidic devices

Because microfluidic systems are characterized by low Reynolds numbers, no turbulent flow is present to enhance mixing within a microfluidic system, and so simple diffusion adequately describes the transport of diffusive species within a microchannel. Simple—or Fickian—diffusion is described by

$$J = -D(\frac{\partial C}{\partial x}) \quad (1)$$

where J is the diffusive flux, D is the coefficient of diffusion for a chemical species in a given medium, and C is the concentration of the chemical species.

The relationship

$$x^2 = 2Dt \quad (2)$$

describes the mean-square displacement of a particle in relation to time lapsed in the system. Because time depends on the square of displacement, diffusion on the microscale is much faster than diffusion on the macroscale. In order to illustrate the effect of scale on diffusion time, consider two observers in a room with a jar of sulfur. Observer one is positioned 10 micrometers away from the jar, while observer two is positioned one million times farther away at 10 meters from the jar. At $t = 0$, the jar is opened and at t_1 the sulfur molecules (and odor) reach observer one at 10 micrometers. At t_2 the sulfur molecules reach observer two at 10 meters. Considering only Fickian diffusion as a method of transport and making use of equation (2), it would take 10^{12} times longer for the molecules to reach observer two at 10 meters as it would to reach observer one at 10 micrometers. Using a realistic diffusion coefficient of 0.16 cm^2sec^{-1} for sulphur in air, observer one would smell the sulphur in 30 nanoseconds while observer two would be spared for 8 hours and 40 minutes. Of course in reality, an observer on the macroscale would be able to smell the sulfur rather quickly, but that is due to the presence of turbulent flow and thermal gradients which facilitate transport in the air. While relying on diffusion for an experiment at the macroscale would be an either costly or impossible time commitment, diffusion can be a readily leveraged mode of transport at the microscale and within microfluidic devices.

PDMS (polydimethylsiloxane) is a commonly used polymer in microfluidics due to its many desirable qualities, including but not limited to optical clarity, biocompatibility, and its ability to be molded down to sub-micron resolution. For this discussion, though, of interest is its high permeability to gas, as it is the most permeable of the elastomeric polymers [10]. Microfluidic experiments for oxygen control frequently involve gas diffusion from a channel through a thin PDMS layer (or membrane) into another area of the device—perhaps another channel or a reservoir.

From Ficks Law, one can determine that, at steady-state and when either side of the membrane is exposed to gas, the permeability P of a polymer membrane to a gas can be described by

$$P = J(\frac{dx}{dp}) \quad (3)$$

where dx is the membrane thickness and dp is the difference in pressure experienced by the two sides of the membrane. From this equation, it is simple to see that diffusive flux

through a membrane will increase with greater pressure difference across the membrane and with decreased membrane thickness.

When considering a typical diffusion membrane in a device as an example, one side of the membrane has gas flowing from a pressurize tank and the other side has ambient air, the diffusive flux experienced by either side is dependent on the net flux of a diffusive species into or out of the membrane. It is important to note that this is really a dynamic process as the gas entering or exiting the membrane can be offset somewhat by sorption to or desorption from the membrane of the same chemical species. At equilibrium, this should result in a constant net flux into and out of the membrane, and the flux through any single step (gas channel to membrane, through the membrane, and membrane to reservoir) is considered the same as the flux through the membrane, and may be defined as

$$J = k_1 \frac{D}{D(k_1 + k_2) + k_1 k_2 dx}(c_1 - c_2) \tag{4}$$

where D is the diffusivity of the gas through the membrane, k_1 and k_2 are the desorption rate constants at each interface of the membrane, and c_1 and c_2 describe the concentrations of the gas in the polymer, according to

$$c = pS \tag{5}$$

where p is the gas pressure on either side of the membrane and S is the solubility of the gas in the polymer. However, when one side of a membrane is exposed to a liquid, this relationship is no longer accurate because gas flux, J, is reduced, and the desorption rate constant of the side of the membrane exposed to liquid, k_2, is different than the rate constant of the side of the membrane exposed to gas, and can now be described by

$$k_2 = \frac{Dk_1}{D + k_1 \triangle x + \rho_w k_1 D} \tag{6}$$

where ρ_w is the wet mass transfer resistance.

In addition to changes in the behavior of sorption and desorption from polymeric membranes depending on the surrounding medium, it is also important to note the differences in the way gas—specifically oxygen for the purposes of this paper—behaves in PDMS versus water. For an excellent in depth analysis, Kim *et al.* present a mathematical analysis of oxygen transport in microfluidic systems[11]. Under identical conditions, oxygen gas is 1.7 times more diffusive in PDMS than in water, and six times more soluble in PDMS than in water[12].

Understanding transport theory aids in designing devices, but to verify oxygen partial pressure several methods for measuring oxygen will be presented in the next section.

3 Methods for measuring oxygen tension in the microenvironment

Measuring oxygen concentration in the microenvironment or within cell cultures presents specific challenges. Samples are not large enough for the Winkler method[13], in which dissolved oxygen (DO) is fixed and measured with stoichiometric methods. Many times, experiments require real time measurement as well as high spatial resolution of oxygen tension. Several tools have been adapted for measuring oxygen tension in the microenvironment, including employing either Clark-style electrodes or luminescent optical sensors.

3.1 Clark-style electrodes

Clark-style electrodes[14] typically use a platinum working electrode and silver chloride reference electrode with potassium chloride for the electrolyte. A voltage of about 800 mV, which is sufficient to reduce oxygen, is applied across the electrodes. Oxygen is reduced at the working electrode, thus producing electrons or current proportional to the amount of oxygen present. The electrodes and electrolyte are protected behind a gas-permeable layer of polytetrafluoroethylene (PTFE) to prevent adsorption of proteins or interfering ions from fouling the electrodes. Because Clark-style electrodes consume oxygen in order to detect it, stirring of the sample is usually required for fast response measurements. The electrode is also very sensitive to changes in sample temperature. Clark electrodes are unreliable for long-term measurements for a number of reasons which contribute to unstable readings: depletion of the electrolyte, the production of OH^- ions affecting the pH causing zero drift, and the anode becoming coated in AgCl. If used with biological samples, the protective, PTFE membrane will also lose permeability over time due to the adsorption of protein and other residues. Clark-style electrodes also suffer from low temporal and spatial resolution due to the time it takes for oxygen to diffuse across the PTFE membrane and to the electrodes. In addition, the relative size of these probes ($\sim$3+ mm diameter probe) makes interfacing with microfluidic channels problematic.

3.2 Luminescent optical sensors

For microfluidic systems, optical oxygen sensors are the tool of choice. They have several advantages over Clark-style electrodes. They do not consume oxygen so they can be used in low or no flow environments and do not suffer from fouling, making them stable for long-term studies. Where Clark electrodes require an electrical connection to each position to be measured and only provide a single, low spatial resolution measurement, optical sensors allow measurement over the entire area of the sensor and at any number of discrete points.

These sensors take advantage of oxygen-indicating fluorophores that are quenched in the presence of oxygen. The degree of quenching is determined by the oxygen partial pressure. The relationship between intensity and oxygen partial pressure is described by the Stern-Volmer equation:

$$\frac{\tau_0}{\tau} = \frac{I_0}{I} = 1 + K_q \tau_0 [O_2] \quad (7)$$

where I_0 and τ_0 are the intensity and excited state lifetime in the absence of oxygen, τ is the excited state lifetime in the presence of oxygen, $[O_2]$ is oxygen concentration, and Kq is the quenching constant. A Stern-Volmer calibration curve must be made for each sensor and application. When a sensor is calibrated, a corresponding Stern-Volmer curve is created by measuring the intensity at no fewer than two known oxygen partial pressures. The intensity data collected is fitted to the Stern-Volmer equation to elicit the corresponding oxygen partial pressure (Figure 1). Typically, a basic fluorescent microscopy setup is sufficient to monitor a fluorescent sensor-equipped device, although custom excitation/detector modules can also be created for portability, miniaturization, or placement in an incubator[15]. Fluorophores are sensitive to photobleaching, where the intensity becomes attenuated after long term constant excitation, but short periodic exposures are typically used to avoid photobleaching. In addition to simple intensity-based measurements, fluorescence lifetime imaging microscopy (FLIM) uses a modulated excitation source and detects the decay in intensity in either the time or frequency domain. This method can be used to reduce background luminescent artifacts, sensitivity to ambient light sources, and variations in intensity due to the concentration of the dye[16].

There are two main types of oxygen indicating fluorophores: ruthenium-based and metalloporphyrin-based. Oxygen-indicating fluorophore dyes such as these can be incorporated into sensors and probes to fit many applications. The simplest method may be directly flowing a suspension of 1 mg/ml of Ruthenium tris(2,2-dipyridyl) dichloride hexahydrate (RTDP) through the device channels. This allows measurement of oxygen tension throughout the entire fluidic network. Although ruthenium based dyes are toxic, this has been performed in live mammalian cultures with less than 10% mortality for 5 hours of exposure[17,18].

To avoid adding toxic dye into culture media, the dyes can be permanently incorporated into a polymeric matrix and embedded into channel walls or features. A thin film platinum(II) octaethylporphyrin ketone (PtOEPK) sensor can be made by dissolving polystyrene in toluene (35% w/w toluene/PS), then adding 0.5 mg/ml of PtOEPK and mixing on a shaker for several hours. A small amount of this solution can be spin coated onto a glass slide. The toluene is then allowed to evaporate leaving PtOEPK in a thin PS layer. This PS/PtOEPK sensor can be cut and installed in regions where oxygen tension measurements are to be taken[19,20]. Oxygen indicating dyes can also be incorporated into a fiber-optic probe. The fluorophore is housed in an oxygen permeable construct at the tip of a fiber optic probe. With a proper optical setup, excitation and detection can now be performed through the fiber. Oxygen can be monitored by placing the fluorophore-doped tip in the sample or network. The advantage of fiber optic oxygen sensors is they can be moved within the sample during measurements and be reused. Park et al. developed fiber optic probes with submicron tips with the intention of monitoring intercellular and intracellular oxygen. The sensors were made by dipping the silica fibers into PtOEPK/PVC dissolved in tetrahydrofuran (THF)[21].

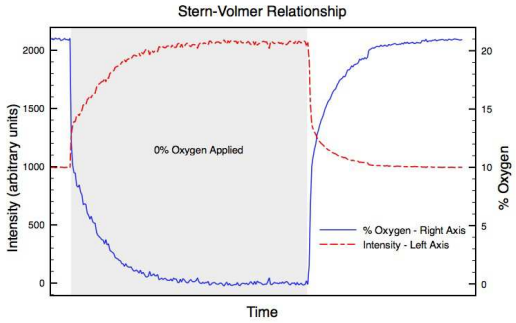

Fig. 1 Example calibration data. This plot demonstrates the response in luminescent intensity of a PtOEPK thin film due to application of a 0% oxygen environment (100% nitrogen). The sensor is first exposed to 21% oxygen atmospheric mix (initial white region), then a 0% oxygen environment is applied by flowing 100% nitrogen over the sensor (grey region). As oxygen is purged, the intensity of the sensor increases due to decreased quenching (red dotted line). The 0% oxygen environment is flushed out with a 21% oxygen mix resulting in a decrease in intensity to the initial level (rightmost white region). The Stern-Volmer relationship is then used to calculate and plot the corresponding oxygen percent (blue solid line).

With transport and detection of oxygen aside, conventional methods for controlling oxygen for research will be discussed next.

4 Methods for global oxygen control of macroenvironments

To study cellular behavior in low concentrations of oxygen, hypoxic chambers, workstations, and perfusion chambers have been the most widely used tools to create hypoxic environments. Unfortunately, these tools offer a single choice of a hypoxic level at a time. The homogeneous oxygen levels provided also do not replicate oxygen gradients found in

vivo which form from radial and axial diffusion of oxygen from the microvasculature and metabolic consumption of oxygen by surrounding cells. Ultimately, the single oxygen level macroenvironments in such culture systems do not establish oxygen gradients that are physiological.

Hypoxic chambers. Hypoxic chambers remain as the tool of choice for imposing variable oxygen conditions because they are small enough to be housed inside a standard incubator, do not require specialized equipment for operation, and have the added advantage of being inexpensive (∼$500) as compared to hypoxic workstations (∼$50,000). Their price has made hypoxic chambers an attractive tool for labs interested in studying cells in low oxygen tension but not necessarily specializing in hypoxia. The hypoxic chamber consists of a vessel in which to place cell culture plates and dishes that can then be purged with a gas mixture of interest, sealed, and placed in an incubator. However, hypoxic chambers are prone to leaks, are inherently low throughput, require considerable incubator space, cannot replicate anoxic conditions even when purged with nitrogen, equilibrate slowly (on the scale of several hours), and are not compatible with microscopic analysis. Additionally, the oxygen level within a hypoxic chamber is imprecise. The oxygen concentration is not stably the same concentration as the infused gas throughout the chamber as transport limitations create a discrepancy between the gas concentration within the infused headspace and the gas concentration at the bottom of the culture dish.

Hypoxic workstations. The hypoxic workstation is a relatively large, sealed biosafety cabinet purged with a gas of interest, monitored with oxygen sensors, and equipped with its own incubator in one corner of the cabinet. Due to its cost, the hypoxic workstation is generally only found in labs specializing in hypoxia research. A workstation is attractive because, as compared to the hypoxic chamber, it is equipped with a small, gas-modulated bench top to perform conventional biological assays such as western blot and PCR preparations. The workspace is useful because hypoxic factors, like the HIF family of transcription factors, degrade rapidly upon re-equilibrating with atmospheric oxygen. Therefore, performing such assays in a sealed, hypoxic environment is ideal to achieve the best results. Atmospheric equilibration is a concern when using hypoxic chambers, rather than hypoxic workstations, as they must be opened to retrieve cell culture contents or even to change media, forcing equilibration with ambient surroundings and an unintended intermittent hypoxia exposure which has been found to alter cell fate and function[22,23].

Though the workstation offers a precisely controlled, homogeneous oxygen environment and space to perform biological assays, the setup is cumbersome. Small, delicate manipulations must be done from outside the cabinet while wearing bulky, integrated rubber gloves. Additionally, like the hypoxic chamber, the workstation cannot be easily coupled to live-cell microscopy unless a microscope is housed within the incubator. Overall, the hypoxic workstation is expensive and leaves too large of a footprint to be readily accessible to a wide population of researchers.

Perfusion chambers. Another option is a commercially available perfusion chamber in which oxygen concentration is able to be modulated by alternating the flow of oxygenated and deoxygenated liquid that is mixed to defined ratios through the chamber. Like the hypoxic chambers and workstations, perfusion chambers lack spatial control. The effect of the added shear stress that comes along with the flow must also be considered with use of perfusion chambers. Shear stress is known to alter cell morphology and gene expression[24–26], so the consequences of non-negligible shear stress should not be underestimated.

Microfluidic platforms have been developed to overcome the inherent limits of these current methods, including lack of spatial control, slow equilibration, and unachievable or difficult coupling to live-cell microscopy. The various applications made possible by microfluidic systems are the topic of the following sections.

5 Local and complex oxygen control of microenvironments

These different methods for oxygen control have been applied to different biological systems, and serve purposes outside of solely controlling oxygen concentration, ranging from improving the quality of an experiment, to creating a more physiologically realistic environment in which to grow cells, to studying the mechanisms of different diseases. Several variations of microfluidic platforms have been used to generate the desired oxygen environment for these experiments, including devices that rely on diffusion from fluid, utilizing on-or-off-chip mixers and equilibration steps, leveraging cellular oxygen uptake to deplete the oxygen, and using chemical, electrolytic or photocatalytic reactions to produce oxygen directly on chip. Microfluidics platforms have been used to control the oxygen microenvironment and to measure the effect of oxygen concentration on biological materials in a variety of ways, including exposing biological specimens to various constant concentrations of oxygen, discrete regions of different oxygen concentrations, and oxygen gradients. Microfluidic systems for controlling oxygen at the microscale have been applied to address a variety of physiologically relevant questions, for examining the behavior of cells in different and tightly-controlled oxygen environments, and they have been applied to studying specific pathologies including cancer, stroke, and sickle cell disease.

5.1 Diffusion from a source fluid

Perhaps the most popular and straightforward method for oxygen control in microdevices is by diffusion from a source or control channel across a thin, gas-permeable PDMS membrane and into the cell culture region. The source fluid in the control channel rapidly diffuses to control the dissolved gas environment experienced by the cells.

5.1.1 Equilibrated liquid. Exposing cells and tissues to different oxygen levels can be accomplished by flowing a pre-equilibrated liquid through the device's control channels. In many cases, media is equilibrated with the appropriate gas before introducing it to cultures. For instance, a commonly used method to mimic the induction of hypoxia is to place cell cultures in medium that has been bubbled with nitrogen[27]. The equilibration of media with nitrogen is frequently done in addition to housing the cultures in a hypoxic chamber or gas-controlled incubator[28] to reach even lower levels of oxygen. In microfluidic systems, cell culture media is also frequently equilibrated with appropriate gas mixtures to control oxygen content. In these systems, constant perfusion of the equilibrated media is usually necessary to maintain the desired oxygen level. Without an ideal, closed system, the oxygen concentration of media will re-equilibrate with ambient surroundings (i.e. the atmosphere) over time.

One example is the work by Grist *et al.* where diffusion from liquids was used to establish oxygen gradients across a central channel. To create the on-chip oxygen gradient, off-chip gas bubbling flasks produced deoxygenated and oxygenated water which was fed via oxygen-impermeable tubing into designated control water channels (Fig. 2). A deoxygenated control water channel flanked one side of a media perfusion chamber containing cells while an oxygenated water channel flanked the other side. Only a thin, PDMS membrane of $\sim$100 μm separated the control water channels from the cell chamber. The high gas permeability of PDMS and the difference in the oxygen level in the control water channels allowed for the spatial gradient generation in the cell chamber. The perfusion rate of the oxygenated or deoxygenated water (100 μL/min) was maintained by syringe pumps which withdrew media, creating negative pressure to pull the liquid through the device. The media perfusion rate in the cell chamber was purposely maintained at a value several magnitudes lower (0.3 μL/min) than the control water channels to permit the formation of a stable oxygen gradient in the cell chamber.

Integrated PtOEPK sensors monitored the oxygen gradient and simulation modeling was undertaken to predict the oxygen gradient profile. However, the model did not fit the acquired data. Namely, the range of oxygen concentrations created experimentally was not as large as that predicted in the simulation. It is suggested that this discrepancy was due to the gas-permeable nature of PDMS and the rapid re-equilibration

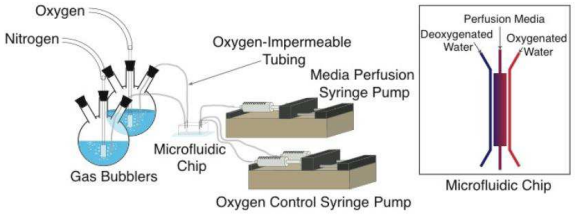

Fig. 2 Example of off chip bubbling experimental setup. Reproduced with permission from ref. 29.

of the device's channels with the ambient partial pressure of oxygen. The researchers expect that coating the outside of the PDMS block with an oxygen-impermeable coating (e.g. with Parylene) could improve oxygen control[29].

5.1.2 Gas perfusion. Flowing gas directly though the control channels eliminates the need for the pre-equilibration of liquid off-chip. Gas also has the advantage of having a lower viscosity than water allowing for more rapid mixing. Additionally, flow is driven with large pressurized sources (gas tank) eliminating the need for syringe pumps. The convenience and simplicity of gas perfusion makes it an easy choice for researchers wishing to accomplish more complicated experimental schemes discussed in detail below. The following devices demonstrate oxygen control in a variety of ways, including discrete control (obtaining multiple, uniform oxygen concentrations), spatial control (binary oxygen concentrations, and spatial gradients of oxygen concentrations), and temporal control (switching between oxygen concentrations at set time intervals or maintaining a constant oxygen concentration over time).

Leclerc *et al.* present an early demonstration of oxygen modulation in a microfluidic device. The system is a bioreactor composed of four microfluidic cell culturing regions stacked one on top of the other, with a media perfusion channel providing flow to the cell culture chamber. Inserted into the middle of the bioreactor (flanked above and below by two cell culturing regions) is what the authors call an "oxygen chamber," which is connected via channels to the environment outside of the bioreactor [Fig. 3]. This served as a way to allow gas from the outside environment to easily modulate the oxygen conditions within the culturing chamber. After culturing, this oxygen chamber design resulted in a 5-fold increase in cell growth compared to a 2-layer bioreactor and 8-fold increase compared to a 4-layer bioreactor without the oxygen chamber. Additionally, albumin production was monitored from cultured hepatocytes and only the cells grown in the 4-layer bioreactor with the oxygen chamber showed increased albumin production over a 12-day experiment[30]. Although the oxygen modulation is completely passive in this device, it represents a conceptual prototype for the more intricate con-

trol devices to follow.

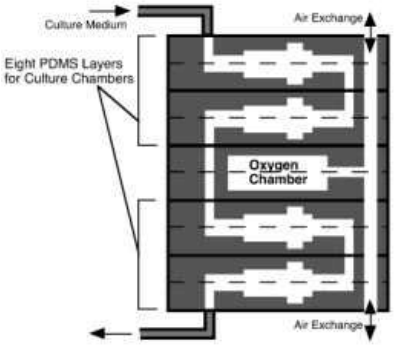

Fig. 3 Early microfluidic bioreactor demonstrating enhanced oxygen modulation. Reproduced with permission from ref. 30.

5.1.2.1 Discrete series of constant oxygen concentrations. A number of devices exist for exercising discrete control of oxygen levels in a microfluidic platform. These devices may be designed such that one device contains several isolated regions of discrete oxygen concentrations, or such that they maintain constant oxygen concentrations over a period of time. Vollmer *et al.* presented a system for dynamic delivery and sensing of oxygen in perfusing medium when oxygen is delivered via a gas channel. PtOEPK oxygen sensors are placed in etched wells of a glass slide at the inlets and outlets of a microfluidic network to monitor oxygen levels. A custom excitation/collection module was created to house the device and monitor oxygen levels from the sensors. Again, oxygen diffuses from a gas channel across a PDMS membrane and into liquid channels. While this system is not applied to biological studies, it is an early example of the use of *in situ* PtOEPK sensors for oxygen characterization, and is a major advance in the development of microfluidic platforms for oxygen control of the microenvironment[20].

Polinkovsky *et al.* present two devices in which individual growth chambers within two microfluidic devices take on discrete values ranging linearly between 0 and 100% oxygen concentration over nine chambers in one device, and exponentially from 0 to 21% oxygen concentration over nine channels in the second device. (Fig. 4) In these experiments, Ruthenium dye was used to characterize the oxygen levels. For each device, the oxygen concentrations in the gas channels are achieved by flowing two gases through a three-step on-chip mixing channel network, culminating in nine separate channels of discrete concentration that flow over the growth chambers, which contain media. The growth chambers can be used to culture yeast, bacteria or mammalian cells, and for the purposes of this experiment, E. coli division rates as a function of oxygen concentration were determined[31]. This device is interesting and useful because it presents a way to use one device to deliver many oxygen concentrations, and this in conjunction with multiple growth chambers means that high-throughput oxygen-controlled experiments can be conducted.

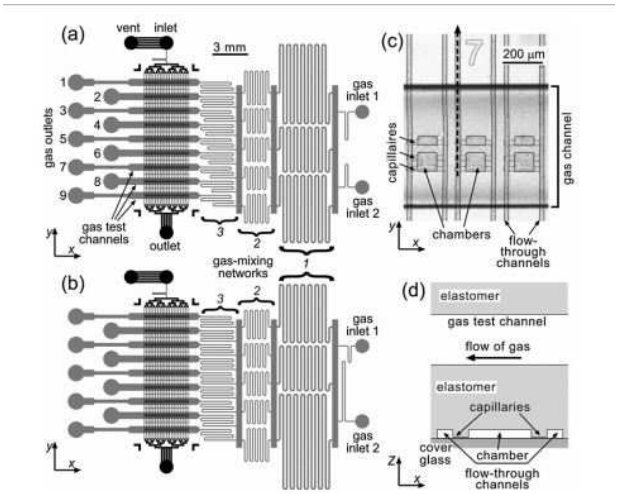

Fig. 4 Two devices for generating discrete series of gas concentrations in chambers for various cultures. In the drawing of the two devices in (A) and (B) the gray serpentine mixing channels determine the dissolved gas environment of the culture region (black vertical channels). The individual lengths of the serpentine channels vary in the two devices to determine the degree of mixing from the two gas inlets. Reproduced from ref. 12.

Lam *et al.* present a microfluidic platform for culturing aerobic and anaerobic bacteria and mammalian cells. An on-chip mixer creates a series of discrete oxygen concentrations by mixing oxygen and nitrogen that range linearly from 0 to 42%, and cells were cultured in channels at these oxygen concentrations. Incorporated into the device is a valve multiplexer, which was used to replace media in each of the eight wells at regular intervals. A custom excitation module was designed using LEDs as the excitation source and paired with a custom infrared detection module. PtOEPK polystyrene sensors were embedded in wet-etched wells of a glass slide. The sensors were calibrated using water with different concentrations of oxygenated water and correlated with the Stern-Volmer analysis. Cell density and growth rates were studied with *E. Coli, A. Viscosus, F. Nucleatum*, and embryonic fibroblast cells[15]. This device couples oxygen and valve control, and demonstrates that techniques necessary for cell culture (media replacement, in this case) can be incorporated into these experiments.

5.1.2.2 Constant oxygen concentration. In addition to microfluidic culture chambers of custom microfluidic devices, Oppegard *et al.* developed a microfluidic insert for a standard 6-well plate, which can be used to modulate oxygen concen-

tration in cell culture in lieu of a hypoxic chamber, and with better oxygen control than a hypoxic chamber. The device's oxygen concentration is characterized using a ruthenium-coated substrate, and was further validated by monitoring HIF-1α expression in cells, to ensure that it agreed with expression levels from traditional methods. The device is an insert which nests into a standard six-well plate, leaving a designated gap from the bottom of the plate. Gas is constantly perfused across the gas-permeable membrane (PDMS) where it diffuses to oxygenate or deoxygenate the multiwell plate at the culture surface. The oxygen concentration within the device rapidly changes when the input gas is changed, and can maintain a steady oxygen concentration over five days [32]. The main innovation of this work was adapting microfluidic oxygen control to the 6-well plate which is a standard workhorse of biomedical research. In a follow-up paper they expanded on this theme to develop an insert for Boyden chambers which also nest into a multiwell plate for cell migration studies (Fig. 5). The ability to maintain an oxygen concentration in conjunction with the ability to adjust to a new oxygen concentration quickly when a new gas is flowed through the device makes it very useful for both constant oxygen concentration studies as well as intermittent hypoxia studies. Hypoxia studies were conducted using an invasive breast cancer cell line and it was found that intermittent hypoxia resulted in different migration than constant hypoxia [33].

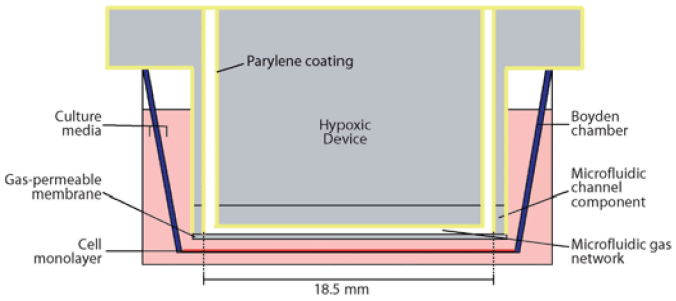

Fig. 5 Oppegard et al. microfluidic insert for 6-well plate with Boyden chamber. Reproduced from ref. 33.

Abaci *et al.* present a microbioreactor for consistent, long-term oxygen control of the microenvironment with live computer monitoring of oxygen concentration in the device. The format of the device is a top gas channel which is used to diffuse oxygen into a lower, closed culture channel via a PDMS membrane. Both channels are etched into polymethylmethacrylate (PMMA). Fluorescent sensors were used to monitor the device's dissolved oxygen level. The system is composed of sensor patches (flat 3*mm* discs), fiber-optic guides, and a 4-channel transmitter device which interfaces with a computer. Figure 6 shows a schematic of the device. Media was constantly perfused at a relatively slow flow rate of $0.02ml/h$. The temporal responses of the oxygen tension in the channel in static conditions in which the gas channel was supplied with discrete oxygen levels (21%, 5%, and 1%) was compared to dynamic conditions which utilized the same discrete oxygen levels in the gas channel but also media perfusion in the culture channel at 0.5 ml/h were compared, and resulted in similar oxygen profiles. The shear stress introduced by perfusion was negligible compared to shear stress levels reported to affect cell behavior. To demonstrate the bioreactors abilities, fibrosarcoma cells were cultured and cell viability, cell density, and circularity tests were performed at 1% and 21% dissolved oxygen concentrations [34].

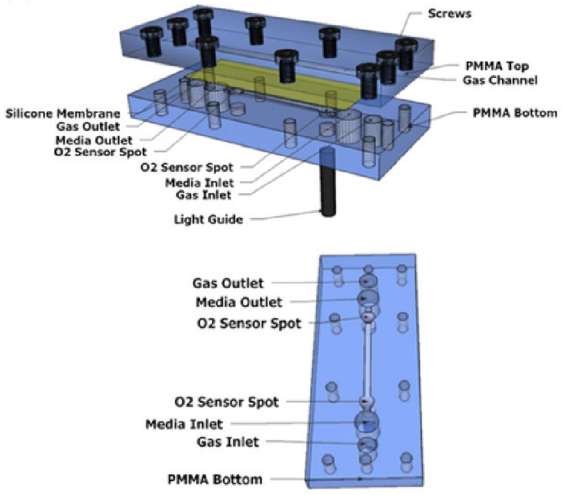

Fig. 6 Microbioreactor with *in situ* oxygen sensors for live computer oxygen monitoring. Reproduced with permission from ref. 34.

Another example of a microfluidic device used to study the behavior of cancer cells in hypoxic and normoxic environments is presented by Funamoto *et al.*, who designed a PDMS microfluidic device with an integrated 3D gel for cell culture flanked by media channels. Each media channel was separated from a gas channel by a 150 μm diffusion gap. Oxygen diffusion between the incubator environment and the PDMS device was inhibited by a polycarbonate (PC) film bonded above the channels. The device was validated using a ruthenium-coated glass cover slip as an oxygen sensor. The device's utility was demonstrated by studying the migration of human breast cancer cells (MDA-MB-231) in hypoxia. Time-lapse live-cell 3D confocal imaging was acquired to determine the cancer cell migration within the gel extracellular matrix (ECM). Cells in the gel showed increased net displacement, total path length, and their ratio (persistence) increased under hypoxia as compared to normoxia. Despite demonstrating that the device de-

sign lends itself to establish a gradient across the gel, cells were not studied in a gradient. Increased migration corresponds with increased invasive behavior of breast cancer cells reported in other studies[35].

In another example, oxygen was used to control the polymerization of sickle-cell hemoglobin (HbS) blood as a model of a vaso-occlusive crisis in sickle cell disease. Again, gas diffuses from a gas channel, across a PDMS membrane, and into the blood perfusion network. Occlusive and relaxation events due to HbS polymerization and depolymerization, respectively, are measured as a function of oxygen concentration by monitoring blood flow velocity in their microfluidic device. The device is presented as a tool to study sickle cell disease and possible future clinically useful agents to block HbS polymerization. CO binding is used to demonstrate that HbS polymerization can be blocked even in cases of extreme deoxygenation[36]. This device represents the first model of the dynamic sickling process without influences of endothelial cells and a follow-up study will be discussed in a later section.

Lo *et al.* demonstrate a diffusion from gas device for a live mouse wound healing study. The device was designed for a live active mouse to wear the device as a topical oxygen therapy method. 100% oxygen was delivered to the device where it diffused across a 100 μm PDMS membrane placed in conformal contact with the wound. The study demonstrated improved collagen maturity in treated mice, although the oxygen therapy did not improve wound closure rates, or microvasculature development[37].

5.1.2.3 Binary oxygen environment. For some experiments, a binary oxygen concentration profile is useful to elicit a biological response as a result of exposure to two distinct oxygen regions. In the previously mentioned paper, Oppegard *et al.* show that an oxygen profile of a dual-condition microchannel can maintain a stable binary oxygen profile over fourteen days. Additionally, the author presents an interdigitated microfluidic channel network that generates a cyclic oxygen profile[32]. Mauleon *et al.* modified an existing brain slice chamber with a PDMS membrane and microfluidic channel layer. This device allows different areas of a 350 μm thick brain slice to be exposed to different oxygen concentrations independently. Oxygen levels and calcium sensitive dyes were used to validate delivery of oxygen to discrete regions of brain slice anatomy[38,39].

5.1.2.4 Oxygen gradients. Diffusion from gas in microfluidic devices can also be used to generate gradients of oxygen concentration within the device. As a continuation of the work previously described by Polinkovsky *et al.*, Adler *et al.* modified this device by controlling input to nine gas channels with computer-actuated three-way solenoid valves, which produce different mixtures to feed to the channels. Additionally, channel wall thicknesses are decreased so different gas concentrations generate a gradient rather than discrete oxygen concentrations. Again, ruthenium dye is used to characterize the oxygen gradient. The authors propose that this device be used to study responses of unicellular organisms to chemotactic gradients, and noted that the device design would allow a user to modify the gradient intensity of specific regions of interest within the device[40].

Most microfluidic oxygen control devices are limited to oxygen control within microfluidic channels, but a demonstration by Lo *et al.* presents gas channels buried within a gas permeable substrate of a larger open well for two different microfluidic networks. One design relies on the diffusion between parallel flow gas channels, and the second design operates via direct mixing of gas in network channels. The oxygen profile generated via the parallel channel device is more linear compared to the mixing network device, from which the profile is strongly sigmoidal (Fig. 7). The devices were characterized using a ruthenium substrate placed directly against the PDMS diffusion membrane. This device was used to determine the reactive oxygen species (ROS) response of cells exposed to 0-100% oxygen gradients. The results indicated ROS response is modulated by oxygen microgradient profiles as expected in hypoxia and hyperoxia[41].

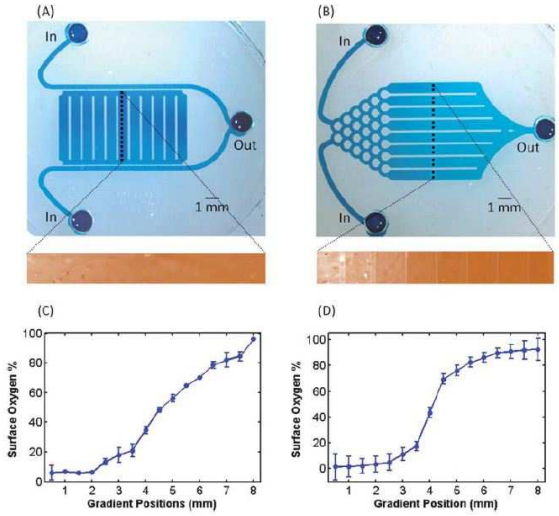

Fig. 7 Lo et al. devices with associated oxygen concentrations. The inlets are supplied with a 100% and 0% oxygen source. Oxygen measurements demonstrate the gradient profiles generated from each mixing design. Reproduced from ref. 41.

5.1.3 Hydration layer. A common disadvantage of controlling gas in microfluidic cell culture systems is evaporation of culture media which is accelerated by the flow of dry gas past the diffusion membrane. Using equilibrated liquids to modulate gas concentrations prevents dehydration but may be

slow and cumbersome if multi-condition or rapid changes in oxygen levels are required. Pre-humidification of gas, by off-chip bubbling, reduces but does not prevent dehydration[42]. A hydration layer is an additional liquid filled channel between the gas layer and culture layer that the delivered gas must diffuse through before it reaches the culture layer. In this way, the gas is humidified directly on-chip as it diffuses to the culture area preventing dehydration.

Wood *et al.* demonstrate the utility of as PBS layer in preventing dehydration of blood while allowing the transport of oxygen in a microfluidic device designed to assess vaso-occlusive risk in sickle cell disease[43]. In cross section, the design stacked a gas channel on top of a PBS channel on top of the blood sample channel (Fig. 8). Oxygen concentration in the gas channel of the chip was modulated with solenoid valves from N_2 and air sources, and oxygen levels were monitored with a fiber optic O_2 sensor at the outlet of the gas channel. Deoxygenation of blood from sickle cell patients resulted in a reduction of flow velocity and blood conductance under the same pressure drop across the device. The reduction of flow velocity is due to the sickle shape adopted by the red blood cells (RBCs) as they became deoxygenated. The molecular basis for the shape change is a variant hemoglobin molecule, HbS, which is the result of a mutation in the gene coding the β-globin protein. Deoxygenation of these RBCs causes HbS to polymerize into long chains which stiffens the cell and leads to the shape change. The morphological change then causes changes in flow by increasing the apparent viscosity of blood, resulting in differences in the rates of change in blood conductance (defined as the velocity per unit pressure drop). The rate of change in blood conductance was leveraged to measure disease severity.

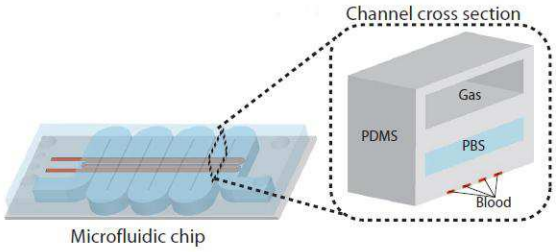

Fig. 8 A hydration layer of PBS between the gas layer and blood layer prevents dehydration of the blood sample. Reproduced with permission from ref. 43.

Cui *et al.* demonstrated what they refer to as a "water jacket" in a device for long-term studies of bacterial cell growth behaviors. An additional layer is added to a diffusion from gas device that serves as a hydration layer. This work also features modeling of humidity within the device due to the hydration layer as well as comparison of dehydration rates in the culture chamber, while using dry gas, humidified gas with an off-chip bubbling method, and their hydration layer with and without humidified gas[42].

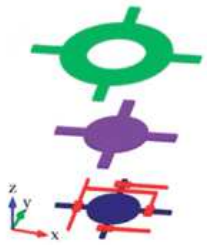

Fig. 9 A hydration layer is incorporated into this device to prevent dehydration of bacterial cell culture chambers. The green layer is gas, the purple is they hydration layer, and the blue is the culture chamber. Reproduced from ref. 42.

5.2 Cellular consumption to deplete oxygen

Simple consumption of oxygen in static cell media is enough to generate hypoxic environments in cell cultures and is dependent on cell density and metabolic rate[44,45]. Sinkala *et al.* cultured Madin-Darby Canine Kidney (MDCK) cells into 500 μm diameter microwells that were embossed into PtOEPK/PS thin films. Cells were seeded at a high density, 330 cells per well, and a low density, 20 cells per well. The PtOEPK/PS wells allowed monitoring of oxygen tension at the culture substrate. The effect of consumption on oxygen levels at the culture surface was drastic for the high seeding density. At the low density condition the oxygen level was measured at 19.5% which is close to ambient levels (21%), whereas at the high density condition the oxygen level was measured 12.6%[19].

Consumption of oxygen by cells can also be combined with constant flow of fresh media to modulate oxygen tension in the microenvironment. In order to study liver zonation Allen *et al.* cultured hepatocytes in a flat plate bioreactor with a 100 μm x 28 mm x 55 mm channel through which media was flowed. The reactor was designed so that cells upstream consumed oxygen leaving less for downstream cells. In this sense, cell media was progressively depleted of oxygen as it flowed through the device. By controlling the oxygen level of media entering the channel and the flow of media through the reactor a steady-state oxygen gradient was formed along the length of cell culture. The gradient could also be shifted along the length of the channel by changing the inlet oxygen partial pressure, and could be made steeper by decreasing the flow rate. This study was performed prior to the development of optical luminescent probes and verification of the gradient was performed with a hypoxia cell assay dye. Also, corresponding inlet and outlet pO_2 levels were shown to correlate

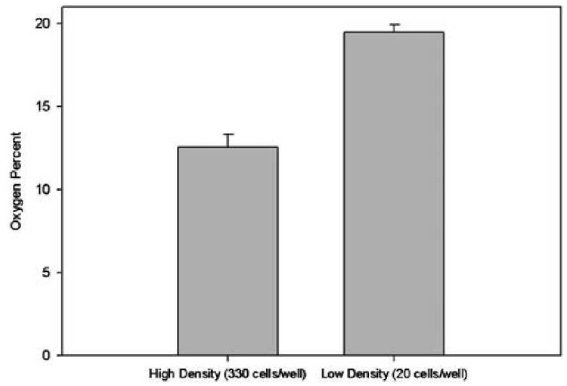

Fig. 10 Effect of cell density on local oxygen microenvironment. The local oxygen level from two cell seeding densities was measured by oxygen sensing culture microwells of 500 μm diameter. MDCK cells seeded at a higher density were shown to deplete the oxygen to a lower level due to a greater rate of consumption. Reproduced from ref. 19.

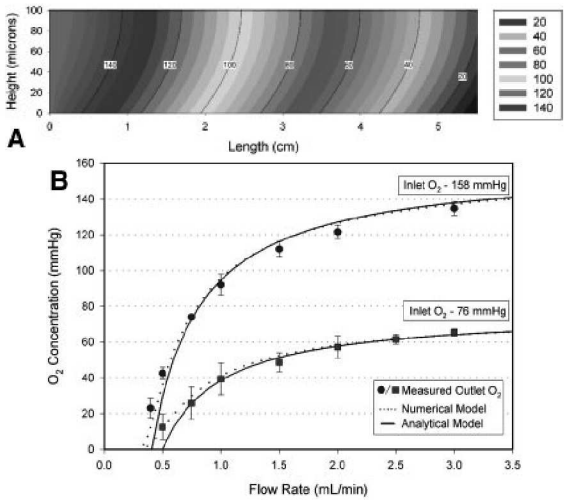

Fig. 11 Modeling of the oxygen gradient in flat-plate bioreactor with dimensions of 28 mm x 55 mm and 100 μm in height. Computational models were created to produce a gradient depending on consumption of oxygen by a cell culture with media of different initial pO_2 levels and flow rates. An example gradient predicted by the model with inlet pO_2 of 158 mmHg and a media flow rate of .035 mL/min demonstrates a linear gradient across the bioreactor as media flow from left to right (A). Measured experimental inlet and outlet pO_2 levels were compared to numerical and analytical model predictions for verification (B). Reproduced with permission from ref. 46.

strongly with model predictions. In addition to validating oxygen levels, they found biological evidence of zonation by the heterogeneous distribution of proteins phosphoenolpyruvate carboxykinase (PEPCK) and cytochrome P450 2B (CYP2B) along the length of the bioreactor, correlating with what is known to occur in physiological oxygen gradients in vivo[46,47].

Mehta *et al.* was the first to use fluorescence lifetime imaging microscopy (FLIM) with ruthenium tris(2,2-dipyridyl) dichloride hexahydrate (RTDP) to detect oxygen tension with living cells in a bioreactor. First this group cultured C2C12 mouse myoblasts in a simple microfluidic channel where pumping was performed in a peristaltic fashion with on chip pin actuators. The oxygen levels of the culture, indicated by FLIM with the ruthenium dye, were shown to decrease proportionally to cell density after a 2 hr incubation time. By using an oxygen indicating fluorophore in the media they were able to verify actual oxygen partial pressures at the culture surface unlike previous consumption dependent studies by Allen *et al.* In a second device Mehta *et al.* also confirmed the generation of an oxygen gradient along a channel that is dependent on flow rate of fresh media as well as the cell density using FLIM[18].

5.3 Generation and scavenging of oxygen on-chip

Oxygen can also be modulated by on-chip reactions that either generate or consume oxygen. The advantages of this method is that it eliminates the need for pressurized gas tanks, although it typically requires syringe pumps to deliver the reagents. It also requires the careful modeling and balancing of reaction kinetics to achieve desired dissolved gas partial pressures.

Skolimowski *et al.* was the first to use an oxygen scavenger to create a gradient in a microfluidic cell culture device. A biofilm of P. aeruginosa was cultured on a thin PDMS membrane below which a serpentine channel carried the scavenger (10% sodium sulfite with 0.1 mM $CoSO_4$ as a catalyst) which irreversibly consumed oxygen from the culture above. A glass slide with a PtOEPK sensor formed the top of the culture chamber and was used to characterize the effect of media flow on the gradient and to monitor oxygen levels of the culture. A media flow rate was chosen to apply a gradient that reduced oxygen saturation at the end of the device by 60% from ambient. Attachment of P. aeruginosa was shown to gradually decrease along the length of the decreasing oxygen gradient[48].

Chen *et al.* took this idea one step further by developing a device that generated and scavenged oxygen on chip using a pair of chemical reactions. The device consisted of a central cell culture channel that is flanked on either side with a chemical reaction channel. An oxygen gradient was formed across the central channel by an oxygen generating reaction, H_2O_2 + NaOCl, and an oxygen scavenging reaction, pyrogallol + NaOH. Each chemical species entered the chip through a dedicated channel, and both respective reactions were initiated on chip by a serpentine mixer just before meeting the cell culture channel. With proper throttling of flow in each chan-

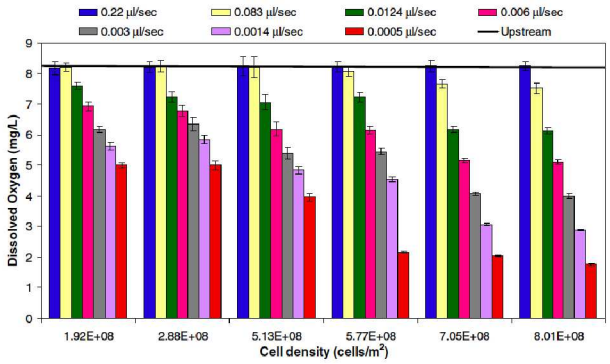

Fig. 12 The relationship between cell density, flow rate and its effect of oxygen depletion in media due to consumption. Reproduced with permission from ref. 18.

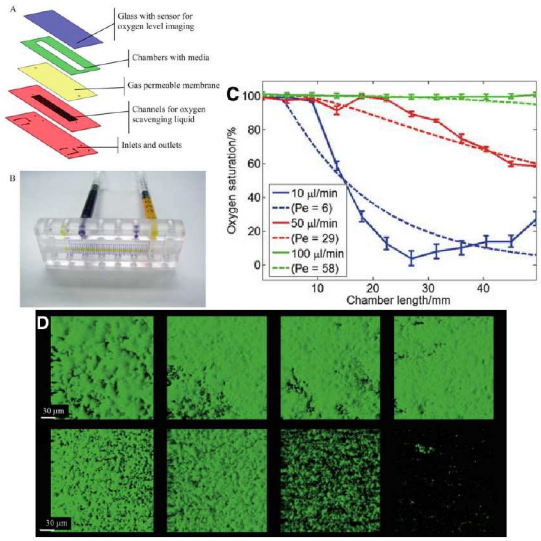

Fig. 13 (A) Schematic of an oxygen scavenging device showing the serpentine channel scavenging layer (red), separated by a thin PDMS layer (yellow) from the culture chamber (green) and the oxygen sensor lid (purple). (B) Image of the device with the serpentine scavenging channel (blue) and culture chamber (yellow). (C) A comparison of simulated oxygen gradients along the chamber (dotted lines) with measured oxygen levels (solid lines) under three different flow rates. (D) Images of stained bacteria in the device at different positions along the gradient. A culture at atmospheric conditions (above) is compared to a culture with a gradient applied resulting in oxygen saturations of 97%, 79%, 60%, and 41% from atmospheric (from left to right). Reproduced from ref. 48.

nel, a steady, linear gradient could be formed across the cell culture and was characterized with a liquid ruthenium-based dye. Carcinomic human alveolar basal epithelial cells were cultured in the device under oxygen gradient and with or without Tirapazamine (TPZ), an anti-cancer drug that is activated to a toxic radical at low oxygen levels, to verify the oxygen sensitive effects on cancer cells[49].

Wang *et al.* demonstrate the formation of an oxygen gradient within a channel by matching the flow of a scavenger with diffusion of oxygen from the surrounding PDMS. With the scavenger flowing through the channel as oxygen diffuses from the PDMS bulk, the result is greater depletion in the center of the channel and ambient conditions near the PDMS walls. The fourth wall of the channel is a glass slide which, because it is gas impermeable, does not contribute oxygen creating a near zero oxygen level for the culture surface. Because the scavenger used is non-toxic (sodium sulfite) cultures of two cancer cell lines were grown directly in the channel and treated with oxygen sensitive TPZ as bio-verification of the gradient[50].

Photocatalytic cells have been explored as a means to oxygenate blood[51–54]. Rasponi *et al.* sought to improve the performance of these devices by scaling it to the microscale where flow could aid in oxygenation. An anatase TiO_2 thin film was deposited onto an indium tin oxide (ITO) thin film to form an TiO_2/ITO semiconducting junction on the surface of a quartz glass substrate. A micro channel molded in PDMS with a platinum electrode deposited as a thin film was bonded over the TiO_2/ITO layer. A bias voltage was applied across the liquid channel between the Pt electrode and the ITO film. The photocatalytic reaction was accomplished by directing UV light through the bottom quartz layer. The rate of degradation of methylene blue was used to characterize the photocatalytic activity of the cell under different flow rates and bias voltages. The device was ultimately tested on bovine blood samples and analyzed with a blood gas analyzer. At a flow rate of 12.5 μL/min, the device was able to increase the saturation of hemoglobin from a venous physiological level of 75.7% to 96.6%[55].

Oxygen can also be generated through water electrolysis. Park *et al.* developed a microfluidic device consisting of a 10 by 10 array of microelectrodes that was able to generate patterned oxygen profiles under a cell culture substrate. A Ti/Pt electrode array of 10 μm square electrodes covering a 1 mm^2 area was deposited onto a glass substrate. A layer molded of PDMS was bonded over the array creating an electrolyte chamber with a cell culture chamber above separated by a thin PDMS layer. The device could be programed to produce a multitude of different patterns and gradients of oxygen across the cell culture area and was characterized with a fluorophore film. The pH of the electrolyte and separation of anode and cathode was kept in a range that discouraged production of peroxides and other reactive oxygen species. Tests demonstrated that a small amount of hydrogen peroxide is produced but its effect on cells would be insignificant. C2C12 myoblasts were cultured in the device in an ambient incubator (21% oxygen) and an anoxic chamber (0% oxygen) and oxygenated at

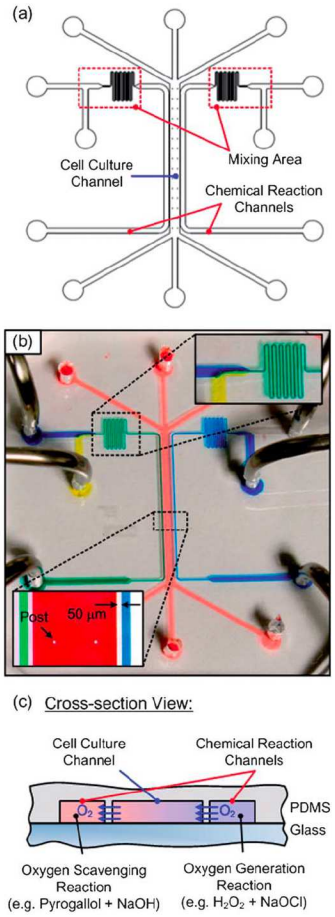

Fig. 14 (A) Schematic of a device that initiates oxygen generating and oxygen scavenging reactions with on-chip mixers and applies an oxygen gradient across a central cell culture channel. (B) Image of the device with the central cell culture channel (red) flanked by the chemical reaction channels (green and blue). (C) a cross-sectional view of the device shows the path of oxygen diffusion from the H_2O_2 + NaOCl channel across the culture channel to the Pyrogallol + NaOH channel where it is consumed. Reproduced from ref. 49.

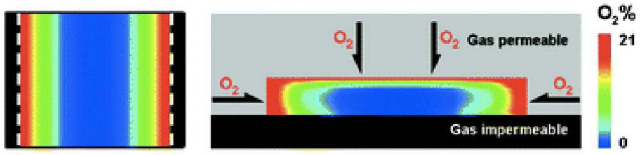

Fig. 15 An oxygen scavenger flowing in a channel creates an oxygen gradient. Oxygen is depleted most in the center of the channel and against the gas impermeable wall and is replenished from the surrounding PDMS bulk. Reproduced from ref. 50.

the same current density and gradient. Due to the device, cells in the ambient culture were subjected to hyperoxia (up to 40% O_2) in different regions and suffered hyperoxic-induced apoptosis. Cells that were cultured in the anoxic chamber and oxygenated with the device were exposed to normoxic oxygen tension (3-20% O_2) and developed healthy cultures demonstrating that the device was not affecting viability, only oxygen levels. Cell viability was confirmed by a Live/Dead assay[21].

6 Conclusions

Proper oxygen partial pressures are important for mimicking physiologically relevant in vivo environments for cell and tissue research. Standard research methods for modulating oxygen in cell culture such as hypoxic workstations and hypoxic chambers suffer a number of disadvantages such as only providing a single uniform condition, having slow equilibration times, and being incompatible with imaging. On the other hand, microfluidics allow for rapid equilibration times, multiple condition, high-throughput parallelization of experiments, and easy imaging capabilities lending itself to oxygen sensitive studies of cells. These devices take advantage of the rapid transport of molecules due to diffusion on the microscale. Microfluidic platforms allow the ability to control the cell culture environment at the microscale including the generation of gradients. Future directions for research in this area may include the study of other relevant oxygen species or gases such as NO, CO_2 and peroxides.

Limitations of microfluidic control of oxygen are shared with limitations of microfluidics in general. While the microfluidic chips are very small they typically require bulky off-chip equipment (ie. gas tanks, syringe pumps, actuator control systems, microscope, etc.). However, microfluidics can better model and create experiments not possible with modern techniques making them a powerful tool in hypoxia research.

References

1 A. Mohyeldin, T. Garzón-Muvdi and A. Quiñones Hinojosa, *Cell stem cell*, 2010, **7**, 150–61.
2 S.-P. Hung, J. H. Ho, Y.-R. V. Shih, T. Lo and O. K. Lee, *Journal of orthopaedic research : official publication of the Orthopaedic Research Society*, 2012, **30**, 260–6.
3 W. K. R. Barnikol and H. Pötzschke, *German medical science : GMS e-journal*, 2012, **10**, Doc11.
4 G. D'Ippolito, S. Diabira, G. a. Howard, B. a. Roos and P. C. Schiller, *Bone*, 2006, **39**, 513–22.
5 Z. Ivanovic, *Journal of cellular physiology*, 2009, **219**, 271–5.
6 L. Basciano, C. Nemos, B. Foliguet, N. de Isla, M. de Carvalho, N. Tran and A. Dalloul, *BMC cell biology*, 2011, **12**, 12.
7 T. Suda, K. Takubo and G. L. Semenza, *Cell stem cell*, 2011, **9**, 298–310.
8 Q. Ke and M. Costa, *Molecular pharmacology*, 2006, **70**, 1469–80.
9 G. L. Semenza, *Trends in Molecular Medicine*, 2001, **7**, 345–350.
10 S. G. Charati and S. A. Stern, *Macromolecules*, 1998, **31**, 5529–5535.
11 M.-C. Kim, R. H. W. Lam, T. Thorsen and H. H. Asada, *Microfluidics and Nanofluidics*, 2013, **15**, 285–296.
12 M. Polinkovsky, E. Gutierrez, A. Levchenko and A. Groisman, *Lab on a chip*, 2009, **9**, 1073–84.

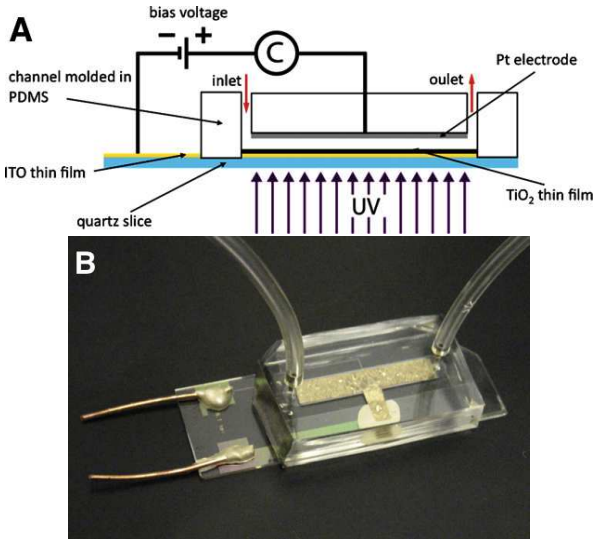

Fig. 16 (A) Schematic of a microfluidic photocatalytic cell that produces oxygen in flowing media. UV light enters the bottom and reacts with the ITO/TiO_2 junction. A microchannel is formed of PDMS and holds a Pt electrode across the channel to which a bias voltage is applied. (B) Image of the device. Reproduced with permission from ref. 55.

13 L. W. Winkler and R. C. Whaley, *The determination of dissolved oxygen in water*, 1888.

14 J. Clark, Leland C., R. Wolf, D. Granger and Z. Taylor, *J Appl Physiol*, 1953, **6**, 189–193.

15 R. H. W. Lam, M.-C. Kim and T. Thorsen, *Analytical chemistry*, 2009, **81**, 5918–24.

16 J. R. Lakowicz, *Principles of Fluorescence Spectroscopy Principles of Fluorescence Spectroscopy*, 2006.

17 D. Sud, G. Mehta, K. Mehta, J. Linderman, S. Takayama and M.-A. Mycek, *Journal of biomedical optics*, 2006, **11**, 050504.

18 G. Mehta, K. Mehta, D. Sud, J. W. Song, T. Bersano-Begey, N. Futai, Y. S. Heo, M.-A. Mycek, J. J. Linderman and S. Takayama, *Biomedical microdevices*, 2007, **9**, 123–34.

19 E. Sinkala and D. T. Eddington, *Lab on a chip*, 2010, **10**, 3291–5.

20 A. P. Vollmer, R. F. Probstein, R. Gilbert and T. Thorsen, *Lab on a chip*, 2005, **5**, 1059–66.

21 E. J. Park, K. R. Reid, W. Tang, R. T. Kennedy and R. Kopelman, *Journal of Materials Chemistry*, 2005, **15**, 2913.

22 V. K. Bhaskara, I. Mohanam, J. S. Rao and S. Mohanam, *PloS one*, 2012, **7**, e30905.

23 M. Han, Y. Wang, M. Liu, X. Bi, J. Bao, N. Zeng, Z. Zhu, Z. Mo, C. Wu and X. Chen, *Cancer science*, 2012, **103**, 1058–64.

24 L. A. Dudash, F. Kligman, S. M. Sarett, K. Kottke-Marchant and R. E. Marchant, *Journal of biomedical materials research. Part A*, 2012, **100**, 2204–10.

25 C.-W. Ni, H. Qiu and H. Jo, *American journal of physiology. Heart and circulatory physiology*, 2011, **300**, H1762–9.

26 S. Obi, K. Yamamoto, J. Ando, H. Masuda and T. Asahara, 2012 International Symposium on Micro-NanoMechatronics and Human Science (MHS), 2012, pp. 54–58.

27 C. Holleyman, D. Larson and K. Hunter, *The Journal of extra-corporeal technology*, 2001, **33**, 175–80.

28 L. Wyld, M. W. Reed and N. J. Brown, *British journal of cancer*, 1998, **77**, 1621–7.

29 S. Grist, L. Yu, L. Chrostowski and K. C. Cheung, SPIE MOEMS-MEMS, 2012, p. 825103.

30 E. Leclerc, Y. Sakai and T. Fujii, *Biotechnology progress*, **20**, 750–5.

31 M. Adler, M. Polinkovsky, E. Gutierrez and A. Groisman, *Lab on a chip*, 2010, **10**, 388–91.

32 S. C. Oppegard, K.-H. Nam, J. R. Carr, S. C. Skaalure and D. T. Eddington, *PloS one*, 2009, **4**, e6891.

33 S. C. Oppegard, A. J. Blake, J. C. Williams and D. T. Eddington, *Lab on a chip*, 2010, **10**, 2366–73.

34 H. E. Abaci, R. Devendra, R. Soman, G. Drazer and S. Gerecht, *Biotechnology and applied biochemistry*, 2012, **59**, 97–105.

35 K. Funamoto, I. K. Zervantonakis, Y. Liu, C. J. Ochs, C. Kim and R. D. Kamm, *Lab on a chip*, 2012, **12**, 4855–63.

36 J. M. Higgins, D. T. Eddington, S. N. Bhatia and L. Mahadevan, *Proceedings of the National Academy of Sciences of the United States of America*, 2007, **104**, 20496–500.

37 J. F. Lo, M. Brennan, Z. Merchant, L. Chen, S. Guo, D. T. Eddington and L. A. DiPietro, *Wound repair and regeneration : official publication of the Wound Healing Society [and] the European Tissue Repair Society*, **21**, 226–34.

38 G. Mauleon, C. P. Fall and D. T. Eddington, *PloS one*, 2012, **7**, e43309.

39 G. Mauleon, J. F. Lo, B. L. Peterson, C. P. Fall and D. T. Eddington, *Journal of neuroscience methods*, 2013, **216**, 110–7.

40 M. Adler, M. Erickstad, E. Gutierrez and A. Groisman, *Lab on a chip*, 2012, **12**, 4835–47.

41 J. F. Lo, E. Sinkala and D. T. Eddington, *Lab on a chip*, 2010, **10**, 2394–401.

42 X. Cui, H. M. Yip, Q. Zhu, C. Yang and R. H. W. Lam, *RSC Advances*, 2014, **4**, 16662.

43 D. K. Wood, A. Soriano, L. Mahadevan, J. M. Higgins and S. N. Bhatia, *Science translational medicine*, 2012, **4**, 123ra26.

44 C. H. Cho, J. Park, D. Nagrath, A. W. Tilles, F. Berthiaume, M. Toner and M. L. Yarmush, *Biotechnology and bioengineering*, 2007, **97**, 188–99.

45 S. S. Verbridge, N. W. Choi, Y. Zheng, D. J. Brooks, A. D. Stroock and C. Fischbach, *Tissue engineering. Part A*, 2010, **16**, 2133–41.

46 J. W. Allen and S. N. Bhatia, *Biotechnology and bioengineering*, 2003, **82**, 253–62.

47 J. W. Allen, S. R. Khetani and S. N. Bhatia, *Toxicological sciences : an official journal of the Society of Toxicology*, 2005, **84**, 110–9.

48 M. Skolimowski, M. W. Nielsen, J. Emnéus, S. r. Molin, R. Taboryski, C. Sternberg, M. Dufva and O. Geschke, *Lab on a chip*, 2010, **10**, 2162–9.

49 Y.-A. Chen, A. D. King, H.-C. Shih, C.-C. Peng, C.-Y. Wu, W.-H. Liao and Y.-C. Tung, *Lab on a chip*, 2011, **11**, 3626–33.

50 L. Wang, W. Liu, Y. Wang, J.-c. Wang, Q. Tu, R. Liu and J. Wang, *Lab on a chip*, 2013, **13**, 695–705.

51 R. J. Gilbert, L. M. Carleton, K. A. Dasse, P. M. Martin, R. E. Williford and B. F. Monzyk, *Journal of Applied Physics*, 2007, **102**, 073512.

52 B. Monzyk, E. Burckle and L. Carleton, *Asaio . . .*, 2006, 456–466.

53 A. Subrahmanyam, T. Arokiadoss and T. P. Ramesh, *Artificial organs*, 2007, **31**, 819–25.

54 A. Subrahmanyam, T. P. Ramesh and N. Ramakrishnan, *ASAIO journal (American Society for Artificial Internal Organs : 1992)*, 2007, **53**, 434–437.

55 M. Rasponi, T. Ullah, R. J. Gilbert, G. B. Fiore and T. A. Thorsen, *Medical engineering & physics*, 2011, **33**, 887–92.